Electronic-structure calculations of self-organized PbS-Bi_2S_3-(Ag_2S) (113) twinning superlattices

Z. Ikonić, G. P. Srivastava, and J. C. Inkson
Department of Physics, University of Exeter, Stocker Road, Exeter EX4 4QL, United Kingdom
(Received 17 July 1997)

The electronic structure of natural, self-organized twinning superlattices based on PbS-Bi_2S_3 and PbS-Bi_2S_3-Ag_2S alloys is calculated and discussed. Superlattices based on PbS-Bi_2S_3 are predicted to be semiconductors, having subbands separated by significant minigaps, as in the conventional ''manmade'' superlattices. On the other hand, the two variations of PbS-Bi_2S_3-Ag_2S superlattices that we have proposed calculations on, are likely to be semimetals. Since these self-organized superlattices should boast high stability against interdiffusion and interface roughness problems, we believe they merit further theoretical and experimental research, and may be found to be suitable for possible applications. [S0163-1829(98)07207-5]

I. INTRODUCTION

Semiconductor superlattices at present almost exclusively rely on the periodic modulation of either the crystal composition or the doping along the structure (or on both). Their successful fabrication has been enabled by the development of sophisticated techniques of molecular-beam epitaxy and metal-organic vapor deposition. In recent years an increasing number of reports have appeared on the so-called ''self-organized'' growth of superlattices, which tend to assemble spontaneously, with no need for external intervention. The phenomenon of spontaneous ordering in semiconductor crystals (and in metal alloys) has been observed for quite some time. For example, spontaneous short-period (CuPt-type) ordering is observed in the semiconductor alloys $InGaP_2$ and $AlInP_2$.[1,2] However, with the short period of just twice that of the bulk material, the electronic structure of such systems is far from exhibiting the low-dispersion, narrow minibands, characteristic of superlattices. Longer periodicities are clearly required if the self-organization is to be useful for the purpose of superlattice fabrication. For instance, rather long-period spontaneous ordering, of $\sim$200 Å, may appear in surface layers of semiconductor alloys,[3] resulting in surface superlattices. Among self-organized ''volume superlattices,'' we mention the discovery of sinusoidal composition modulation, with the periodicity $\sim$18–32 Å, in the strained system ZnSe-ZnTe when grown on a misaligned substrate.[4]

There is also the interesting well-known phenomenon of polytypism, as another example of the appearance of self-organization in semiconductors, which is now considered as an alternative route to superlattices.[5–7] Among semiconducting materials polytypism appears in SiC and the (Zn,Cd)(S,Se) system. It may provide a rather long-period modulation of the structure, based on a different principle than that in conventional superlattices: in such cases the zinc-blende and wurtzite phases of the same material are interlaced. A number of different polytypes have been observed, and since their formation energies are very close to each other, it is presently rather difficult to grow a superlattice with a precisely required period.

Related to polytypism is the phenomenon of twinning, recently proposed by us as a possible principle of building superlattices.[8] It comprises the reversal of the atomic stacking sequence along some axis, or, macroscopically, changing the crystal orientation while keeping the composition and doping constant. Twinning is a commonly occurring phenomenon in a number of crystals, including almost all semiconductors. In the case of zinc-blende-type crystals the (111) plane is the most common twinning plane, because such a twin has a very low formation energy as the nearest-neighbor atomic distances and bond angles remain unchanged. (The same is approximately true for twins in rock-salt-type semiconductors.) Although the crystal structure and the material composition are identical on both sides of the twin boundary, the wave-function symmetry mismatch due to the opposite orientation gives rise to considerable electron scattering at the periodically distributed interfaces. Indeed, calculations for Si- or Ge-based,[8] and for PbS-based[9] superlattices indicate a prominent miniband structure. Such superlattices have not been fabricated so far, with a notable exception: a somewhat irregular, but spontaneous twinning ''superlattice'' was observed in free-standing GaAs quantum wires,[10] apparently enabled by surface effects. As for silicon, the successful fabrication of a single twin boundary[12] does not seem to have induced further research efforts towards realization of superlattices.

In this paper we draw attention to another class of self-organized superlattice structures, which are based on twinning induced by chemical composition, i.e., on ''chemical twinning.'' It is interesting to point out that such structures have been known for some time to occur in natural minerals, but have only been studied from the crystal chemistry point of view. Despite the fact that such structures are based on compounds that are individually classified as typical semiconductors (PbS,Bi_2S_3), these have never been considered as semiconductor superlattices, nor has their electronic structure ever been calculated or determined experimentally. An important feature here is that the superlattice-type ordering appears in alloys of PbS and Bi_2S_3 (possibly with Ag_2S or Cu_2S as the third constituent) spontaneously, upon crystallization from the melt, which makes these superlattices self-organized. In this paper we calculate their electronic structure, in order to find whether there are minibands that would make them potentially useful, and definitely interesting for further investigations. A brief report on the electronic band

structure of PbS-Bi_2S_3 superlattices has recently been presented.[11]

II. THE CRYSTAL STRUCTURE

The existence of special compositions of PbS-Bi_2S_3 alloys that form superlattice-type structures was revealed during studies of the mixed lead-bismuth sulfide ore minerals. Subsequently, these natural superlattices have also been grown in the laboratory,[13,14] by either melt recrystallization or by vapor-phase epitaxy. Their crystal structure has been quite extensively studied in a number of papers.[13–18] Only two compositions in the PbS-Bi_2S_3 system are known to exhibit stable periodic structures. The (ideal) compositions $3\cdot$PbS-Bi_2S_3 and $6\cdot$PbS-Bi_2S_3, known in mineralogy as lillianite and heyrovskyte, respectively, were found to form layer structures that could best be described as stacks of oppositely oriented (i.e., twinned) layers of cubic rock-salt-type material of the same chemical composition and same thickness, albeit with slightly more complicated structure of the interface. The bulklike slabs are rotated by 180° in respect to each other about the [113] axis, and joined at the (113) twinning planes (labeled with respect to the cubic unit cell of the underlying material). Viewed as superlattices, the two structures may be classified according to the ratio of the width of the two half-periods and the width of the underlying rock-salt elementary cell in the [113] direction. They may thus be labeled as (n,m) twinning superlattices, with $n=m=6$ and $n=m=9$ for $3\cdot$PbS-Bi_2S_3 and $6\cdot$PbS-Bi_2S_3, respectively. The corresponding chemical formulas per period are $Pb_6Bi_4S_{12}$ and $Pb_{12}Bi_4S_{18}$, respectively. The presence of a small amount of impurities (in the few % range), commonly found in naturally occurring minerals, does not affect the crystal structure. More importantly, admixing a sizable amount of Ag_2S or Cu_2S does lead to a variety of new superlattices, all based on chemical twinning, with different periodicities and internal structures of the unit cell. Structures with unequal thicknesses of both obversely and reversely oriented slabs appear. These include a (6,9) superlattice known as vikingite with formula $Pb_5Bi_6Ag_2S_{15}$, a (6,6) superlattice known as gustavite with formula $Pb_2Bi_6Ag_2S_{12}$, a (11,7) superlattice known as eskimoite with formula $Pb_2Bi_6Ag_2S_{12}$, a (11,7) superlattice known as ourayite with formula $Pb_5Bi_{7.5}Ag_{3.5}S_{18}$, and the largest period (13,13) superlattice known as ourayite with formula $Pb_{7.5}Bi_{10.25}Ag_{6.25}S_{26}$. Among the PbS-$Bi_2S_3$-$Ag_2S$ superlattices some are also found in minerals (and usually have nonidealized compositions), others are synthetized in the laboratory,[18] while those based on PbS-Bi_2S_3-Cu_2S are all synthetic. With a few exceptions, these are less thoroughly studied than $3\cdot$PbS-Bi_2S_3 and $6\cdot$PbS-Bi_2S_3.

A quite simplified explanation of the formation of superstructures in PbS-Bi_2S_3 alloys would be the following. The rock-salt (i.e., PbS-like) structure requires an equal number of metal and nonmetal atoms in the composition. There is a ''shortage'' of metal atoms in the alloy. Thus instead of forming a rock-salt structure with a large number of vacancies, the crystal finds a more favorable way out—to make a superlattice structure with (113) as the twinning plane so that some metal atoms are ''shared'' between nonmetal atoms. The frequency of occurrence of twinning planes depends on the alloy composition and is such that the shortage of metal atoms is exactly compensated for. Attempts to make a (113) twin by cutting and rotating a half of the rock-salt crystal would bring two atoms of the same type too close to each other, and indeed such a twin does not form. It is only the deficiency of metal atoms in the alloy that makes it possible: the ''shared'' metal atom lies exactly at the twin boundary, so that the full structure is not much distorted. However, much about the formation and stability of these structures is yet to be understood. For instance, based on chemical formulas and the periodicities of $3\cdot$PbS-Bi_2S_3 and $6\cdot$PbS-Bi_2S_3, one may naively expect that further decrease of the contents of bismuth in the alloy will result in a structure with an even larger period. Nothing like that has been reported, at least not under the quasiequilibrium growth conditions normally used. Also, recrystallization of a melt with a composition in between that of $3\cdot$PbS-Bi_2S_3 and $6\cdot$PbS-Bi_2S_3 gives a mixture of the two phases, not a new phase. Only in the case of quenching could a thin interphase boundary with ''wrong'' composition or layer width be detected.[14] While some attempts have been made[19] to explain the existence of only these two phases, based on the elastic strain energy, they were not very successful, and this problem apparently awaits a more microscopic approach.

The unit cell of the symmetric PbS-Bi_2S_3 is base-centered orthorhombic. The idealized structure of heyrovskyte $Pb_{12}Bi_4S_{18}$ unit cell is displayed in Fig. 1(a). The two slabs of oppositely oriented rock-salt material joined at the twinning interface in the middle are clearly visible. The sulphur atoms at the interface are at their regular rock-salt positions, but the two adjacent layers lack the metal atoms that would be $1/(2\sqrt{11})$ of the cubic lattice constant away from the interface if they also were at regular rock-salt positions. Instead of these two, there is a single metal atom at the interface, off its normal rock-salt position, which is ''shared'' between nonmetals in the neighboring layers. The two sides of the base of the unit cell would ideally measure $a/\sqrt{2}$ along $[1\bar{1}0]$ and $a\sqrt{22}/2$ along $[33\bar{2}]$, with a denoting the cubic lattice constant, and the third side should be $(n+m)a/\sqrt{11}$ along the [113] direction. The ratio of experimentally determined unit-cell dimensions[14,16,17] deviates very slightly (within 1%) from the idealized value. The $3\cdot$PbS-Bi_2S_3 unit-cell dimensions (in Å) are $4.112\times13.522\times20.608$, and those of $6\cdot$PbS-Bi_2S_3 $4.132\times13.697\times31.355$, with the corresponding effective cubic lattice constants being 5.759 and 5.820 Å, respectively. While ideally all the atoms, except the metal atom at the twinning interface, should occupy the same positions as in rock-salt structure, in reality some amount of atomic relaxation takes place, mostly close to the interface. Relaxed atomic coordinates have been quite precisely determined for both $3\cdot$PbS-Bi_2S_3 (Ref. 16) and $6\cdot$PbS-Bi_2S_3.[17] Figure 1(b) displays the relaxed structure of the $6\cdot$PbS-Bi_2S_3 unit cell, constructed according to the data in Ref. 17, and can be distinguished from the idealized only by slightly nonparallel rock-salt bonds close to the interface. The ordering of the metal atoms in the unit cell (from layer to layer) has also been experimentally determined.[16,17] The ''stacking sequence'' in a period of $3\cdot$PbS-Bi_2S_3 was found to be

$$\widehat{\text{Pb}}\text{-Mx-Mx-Mx-Mx-}\widehat{\text{Pb}}\text{-Mx-Mx-Mx-Mx} \qquad (1)$$

and in $6\cdot$PbS-Bi_2S_3

$$\widehat{\text{Pb}}\text{-Mx-Mx-Pb-Pb-Pb-Mx-Mx-}\widehat{\text{Pb}}\text{-Mx-Mx-Pb-Pb-Pb-Mx-Mx}, \tag{2}$$

where hats denote the positions of interface (twinning) planes, and Mx stands for the 50%-50% mixture of Pb and Bi. Note that both superlattices have two metal atoms less than the total number of layers, because the interface metal is common to the two adjacent layers. No significant ordering of Pb and Bi atoms in the mixed-composition layers in the (113) plane was detected, i.e., they are statistically distributed in these layers.[16,17] In fact, with exactly 50%-50% Pb-Bi composition one may simply construct new unit cells that would have a single type of atom at a site, by doubling the volume, (i.e., the cell in Fig. 1 would then be primitive, of simple orthorhombic type). There are clearly a number of ''double-chain'' stacking sequences of Pb and Bi atoms (i.e., with two atoms per layer) that all lead to the same measured layer compositions. In these doubled cells, however, some of the symmetry possessed by the base-centered orthorhombic primitive cell (''single cell'') is necessarily lost. Consider, for instance the following stacking sequences in the double cell of $3\cdot \text{PbS-Bi}_2\text{S}_3$, with the same average composition of layers as had the original single cell:

$$\begin{aligned}&\widehat{\text{Pb}}\text{-Bi-Pb-Pb-Bi-}\widehat{\text{Pb}}\text{-Pb-Bi-Bi-Pb}\\&\widehat{\text{Pb}}\text{-Pb-Bi-Bi-Pb-}\widehat{\text{Pb}}\text{-Bi-Pb-Pb-Bi},\end{aligned} \tag{3}$$

$$\begin{aligned}&\widehat{\text{Pb}}\text{-Bi-Pb-Bi-Pb-}\widehat{\text{Pb}}\text{-Pb-Bi-Pb-Bi}\\&\widehat{\text{Pb}}\text{-Pb-Bi-Pb-Bi-}\widehat{\text{Pb}}\text{-Bi-Pb-Bi-Pb},\end{aligned} \tag{4}$$

and

$$\begin{aligned}&\widehat{\text{Pb}}\text{-Bi-Pb-Pb-Bi-}\widehat{\text{Pb}}\text{-Bi-Pb-Pb-Bi}\\&\widehat{\text{Pb}}\text{-Pb-Bi-Bi-Pb-}\widehat{\text{Pb}}\text{-Pb-Bi-Bi-Pb}.\end{aligned} \tag{5}$$

While the first two preserve the screw symmetry, the atomic distribution is either nonsymmetric in respect to the twinning plane, or nonsymmetric in respect to the middle of the layers. The third, however, lacks the screw symmetry. In contrast, the single cell with mixed composition layers (1) has all the three symmetries as one would normally except in such a structure. We shall return to this point later on, when discussing the electronic structure calculation.

As for the $\text{PbS-Bi}_2\text{S}_3\text{-Ag}_2\text{S}$–based superlattices, those with symmetric structure of the period also have the base-centered orthorhombic unit cell, and those with asymmetric period have the base-centered monoclinic unit cell (in the case of doubling the volume, for the same reasons as discussed above, these would become simple orthorhombic and simple monoclinic, respectively). The lattice parameters have been determined in a large number of cases,[14] but, as far as we know, the relaxed atomic coordinates and metal atoms ordering was investigated only for $\text{Pb}_5\text{Bi}_6\text{Ag}_2\text{S}_{15}$, and even that for a mineral sample with nonidealized composition.[20] However, data presented in Ref. 20 and trends displayed by the *known* ordering in $3\cdot \text{PbS-Bi}_2\text{S}_3$ and $6\cdot \text{PbS-Bi}_2\text{S}_3$, allow one to infer the probable stacking sequence for $\text{Pb}_5\text{Bi}_6\text{Ag}_2\text{S}_{15}$ (6,9),

$$\widehat{\text{Pb}}\text{-Mx-Bi-Bi-Mx-}\widehat{\text{Pb}}\text{-Mx-Bi-Pb-Pb-Pb-Bi-Mx}, \tag{6}$$

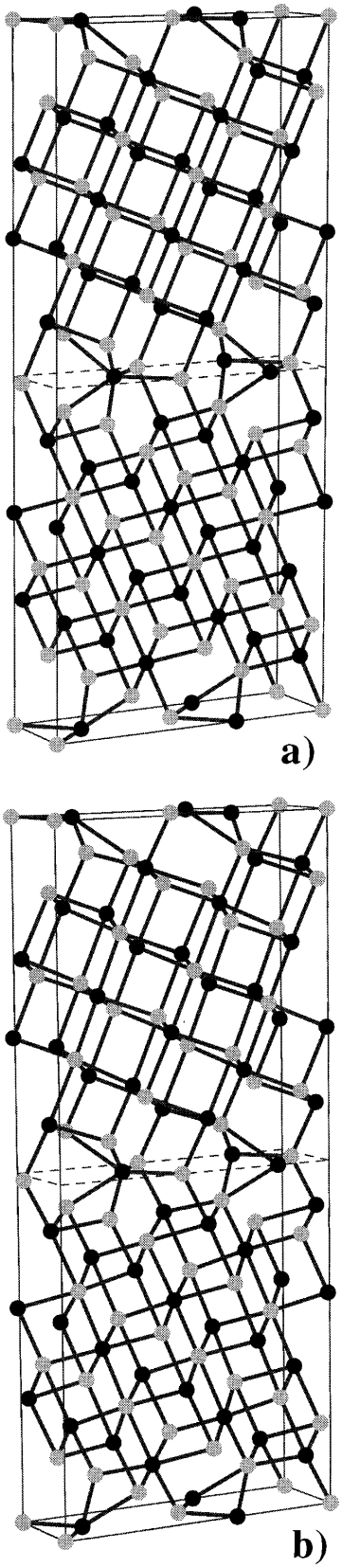

FIG. 1. The idealized (a) and relaxed (b) structure of the (9,9) superlattice (9,9) superlattice (heyrovskyte) unit cell. Light and dark atoms denote sulphur and metal, respectively. The shorter side of the base is along [110], and the longer along [332] directions, and the vertical edge is along the [113] direction of the underlying cubic system. The dashed rectangle outlines the twinning plane (interface).

and, from it, also for $Pb_2Bi_6Ag_2S_{12}$ (6,6),

$$\widehat{\text{Pb}}\text{-Mx-Bi-Bi-Mx-}\widehat{\text{Pb}}\text{-Mx-Bi-Bi-Mx}, \tag{7}$$

where now Mx stands for the 50%-50% mixture of Ag and Bi. Analogously to Eqs. (3)–(5) one may construct various sequences with single atom type at a site for the doubled cells. For instance, in $Pb_2Bi_6Ag_2S_{12}$ these could be, e.g.,

$$\begin{matrix}\widehat{\text{Pb}}\text{-Bi-Bi-Bi-Bi-}\widehat{\text{Pb}}\text{-Ag-Bi-Bi-Ag}\\ \widehat{\text{Pb}}\text{-Ag-Bi-Bi-Ag-}\widehat{\text{Pb}}\text{-Bi-Bi-Bi-Bi}\end{matrix} \tag{8}$$

or

$$\begin{matrix}\widehat{\text{Pb}}\text{-Bi-Bi-Bi-Ag-}\widehat{\text{Pb}}\text{-Ag-Bi-Bi-Bi}\\ \widehat{\text{Pb}}\text{-Ag-Bi-Bi-Bi-}\widehat{\text{Pb}}\text{-Bi-Bi-Bi-Ag.}\end{matrix} \tag{9}$$

The unit-cell dimensions (in Å) for $Pb_2Bi_6Ag_2S_{12}$ and $Pb_5Bi_6Ag_2S_{15}$ are $4.142\times13.504\times19.612$ and $4.112\times13.598\times25.249$, respectively.[14]

III. METHOD OF CALCULATION

To calculate the band structure, we have employed the nonlocal empirical pseudopotential method, within the supercell implementation. The form functions for S and Pb atoms are constructed from data in Ref. 21, and for Bi from Ref. 22. For convenience, all these (in the case of Bi the local part only) were fitted to the standard form $V(q)=a_1(q^2-a_2)/[\exp(a_3(q^2-a_4))+1]$, where $a_{1-4}=(0.208,2.967,2.041,2.720)$ for S, (0.256,2.171,1.343,1.829) for Pb, and (0.818,3.831,0.505, −3.468) for Bi.

The pseudopotential for silver, with its important *d* electrons, requires some discussion. We have started from the set of local form factors and the coefficients for the nonlocal part of the pseudopotential given in Ref. 23. These provide a reasonably accurate description of the silver band structure. The latter turns out to be very sensitive to the precise values of all the parameters, and also depends on the kinetic energy cutoff, and even on the method of matrix diagonalization (e.g., a very similar set of parameters for the pseudopotential from Ref. 24 works properly *only* if one employs Löwdin's method with specified cutoffs of the large and small matrices, but not if full matrix diagonalization with whatever cutoff is employed, as in this work). Attempts to reproduce results of Ref. 23 by using the fitted form function of the above form failed, because it allows only for a monotonically, not oscillatory, decaying $V(q)$ for large q, while Ag seems to demand the later.[23] Thus, for Ag we have fitted the available data to the usual ionic form function $V_{\text{ion}}(q)=b_1(\cos(b_2q)+b_3)\exp(-b_4q^4)$ screened with the Lindhart dielectric function [this enables more than a single zero crossing of $V(q)$]. With the values $b_{1-4}=(-0.2246,2.040,-0.304,0.0)$ the metal Ag band structure was reproduced successfully.

In calculations using empirical pseudopotentials one normally allows for refitting of the parameters initially chosen, by comparing the calculated results for the crystal under consideration with a few *known* experimental (or possibly theoretical) values (of some band gaps, for instance). However, we could not pursue such an approach because, as already noted, there are no measurements or other calculations for these structures that could be used for reference. For this reason, and in view of the fact that much of the structure is rock-salt like, we have only required that the form functions for Pb and S do give the correct band structure of PbS (this is important, since PbS is the major constituent in some superlattices). On the other hand, the pseudopotentials for Bi and Ag were taken as given in the literature.

Next we discuss mixed-composition layers in twinning superlattices. It is a widely accepted practice, when dealing with semiconductor alloys, to use the virtual crystal approximation, which in the pseudopotential-based calculations amounts to using the (linearly) weighted average of form factors at atomic sites occupied by ''mixed'' atoms. On a macroscopic scale, this concept is also employed in the effective-mass type of calculations for finding the band gap and the effective mass in the alloy. Deviations from the linear approximation (Vegard's law) are usually considered to be acceptable, though not negligible. However, in all these applications of the virtual crystal approximation one has the situation that only similar atoms, i.e., of the same valency, may be present at a site. Theoretically it would be much more demanding to model the experimentally determined fact that *dissimilar* atoms, like Pb and Bi, or Bi and Ag, share the same positions in some layers of chemical twinning superlattices.

Since the supercell calculations for superlattices deal with matrices that are large anyway, using the virtual crystal approximation would definitely be desirable. Even for those superlattices where doubling the unit cell alleviates this problem (Sec. II) the computation time would increase by 2^3, i.e., by almost an order of magnitude *for each stacking sequence of metal atoms,* and there may be at least a few worth exploring [e.g., like Eqs. (3)–(5)], with their relative presence in the real system being unknown. For other structures that require more than doubling the unit cell to achieve the single atom type at a site, the situation is even worse. To resolve this problem we have performed a limited number of test calculations of electronic states in PbS-Bi_2S_3–based ($3\cdot$PbS-Bi_2S_3 and $6\cdot$PbS-Bi_2S_3) and PbS-Bi_2S_3-Ag_2S–based ($Pb_2Bi_6Ag_2S_{12}$) superlattices, using both the virtual crystal approximation within the ''single cell'' and the ''double cell'' implementation with configurations like those described by Eqs. (3)–(5). While some results will be given in Sec. IV, here we note only that the virtual crystal approximation was found to be more or less acceptable for PbS-Bi_2S_3–based structures, particularly for $6\cdot$PbS-Bi_2S_3 because errors introduced by it are generally of the same order as those arising from other approximations or uncertainties. In the case of PbS-Bi_2S_3-Ag_2S–based superlattices, however, the virtual crystal approximation leads to large errors and should not be used.

Another way of dealing with the mixed-atoms problem would be to retain the minimum volume primitive cell, while setting up a new stacking sequence of single atoms at a site, and hoping that this would not perturb energies more than do other approximations made in calculation. For instance, prior to measurements reported in Ref. 16, the stacking sequence

$$\widehat{\text{Pb}}\text{-Bi-Pb-Pb-Bi-}\widehat{\text{Pb}}\text{-Bi-Pb-Pb-Bi} \tag{10}$$

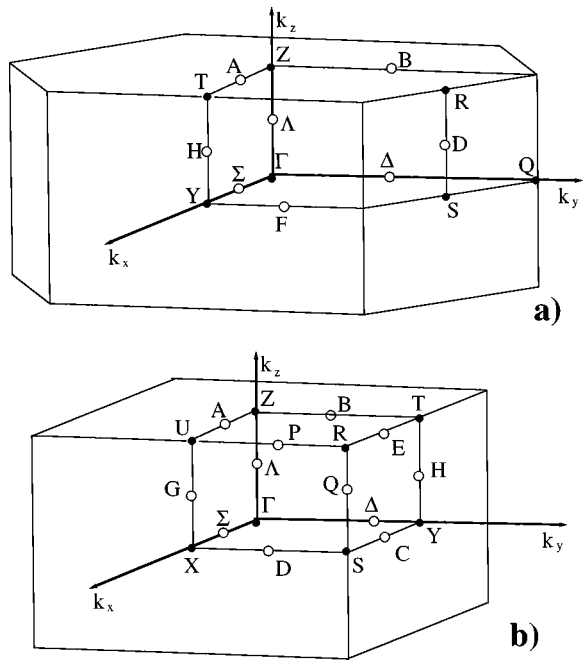

FIG. 2. The first Brillouin zone corresponding to the base-centered orthorhombic unit cell (a), and to the simple orthorhombic unit cell (b), with the irreducible parts indicated.

was considered as ideally ordered $3\cdot$PbS-Bi_2S_3structure.[15] As we demonstrate in Sec. IV, different orderings of metal atoms do induce shifts of states energies of the order of $\sim$0.1 eV, so this approach may also be of some help in calculations.

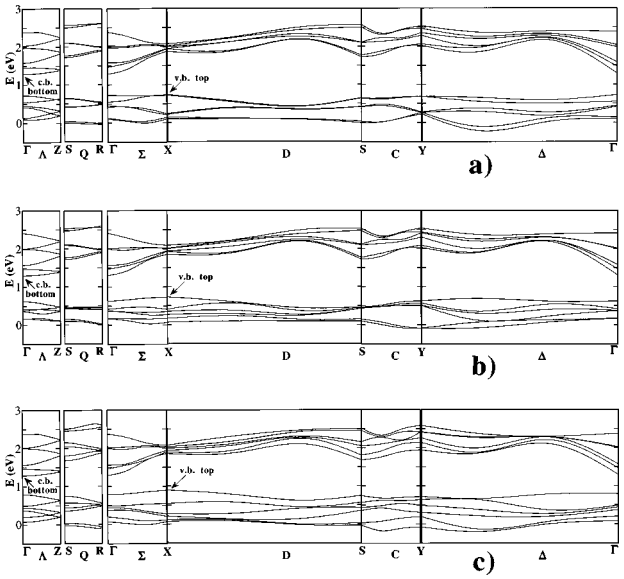

FIG. 3. The dispersion of the six highest valence and six lowest conduction minibands in $3\cdot$PbS-Bi_2S_3 (6,6), along some characteristic directions, calculated within the double-cell approach with configurations described by Eqs. (3), (4), and (5) are given in (a), (b), and (c), respectively. The zero of energy is arbitrary, as came out of calculation, but is the same in all three cases. The atomic coordinates are set at their relaxed measured values (Ref. 16).

The spin-orbit coupling is generally important in compounds with heavy metals, like Pb and Bi. However, in order to limit the size of the problem this effect was not included in the calculations. In fact, the spin-orbit coupling in PbS affects the main band gap by $\sim$0.1 eV, while some remote bands are much more affected. Since our primary interest was in states close to the superlattice band gap, and errors of the order of magnitude 0.1 eV are inevitably present, there was no point in accounting for this effect at the cost of doubling the size of the problem.

In the case of PbS-Bi_2S_3–based superlattices, where the virtual crystal approximation could be used, the first Brillouin zone corresponding to its base-centered orthorhombic unit cell[25] is displayed in Fig. 2(a). However, in case of cell doubling, which has to be used for PbS-Bi_2S_3-Ag_2S–based superlattices and may also be used for PbS-Bi_2S_3 ones; the first Brillouin zone corresponding to the simple orthorhombic unit cell is given in Fig. 2(b). It should be noted that the latter is obtained by the folding in of the former, so that, for instance, the dispersion along the $\Gamma-Z=\Lambda$ and $Y-T=H$ lines (in the superlattice ''growth direction'') of Fig. 2(a) both fold into the $\Gamma-Z=\Lambda$ line of Fig. 2(b), while the $S-R=D$ line of Fig. 2(a) does not fold [but is denoted as $S-R=Q$ on Fig. 2(b)].[25]

The plane-wave basis was chosen, with the kinetic energy cutoff set at 5.1 Ry for PbS-Bi_2S_3–based superlattices (this corresponds to 747 and 1165 plane waves at the zone center for $3\cdot$PbS-Bi_2S_3 and $6\cdot$PbS-Bi_2S_3, respectively). For PbS-

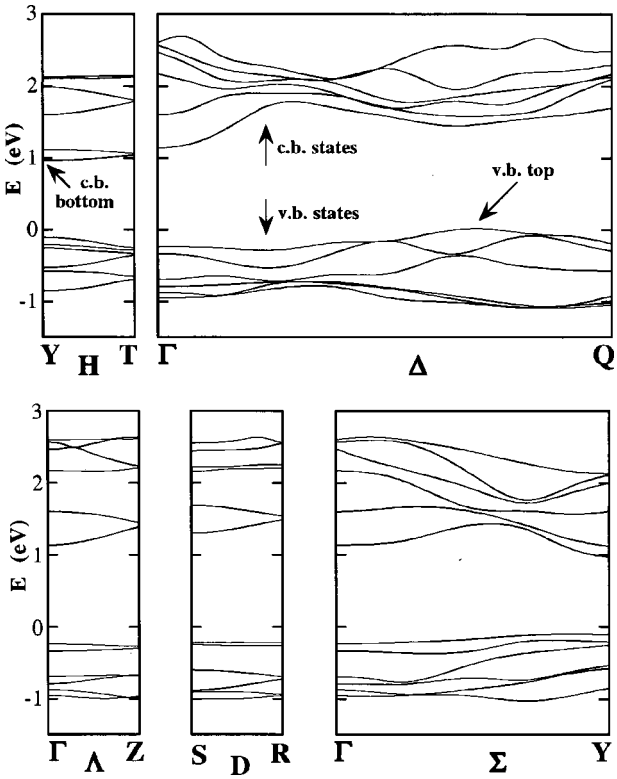

FIG. 4. Same as Fig. 3, but calculated within the single-cell virtual crystal approximation, using the relaxed measured coordinates and atomic ordering described by Eq. (1). Lines H, Λ, and D are along the superlattice ''growth direction'' [113]. The zero of energy is set at the valence-band top.

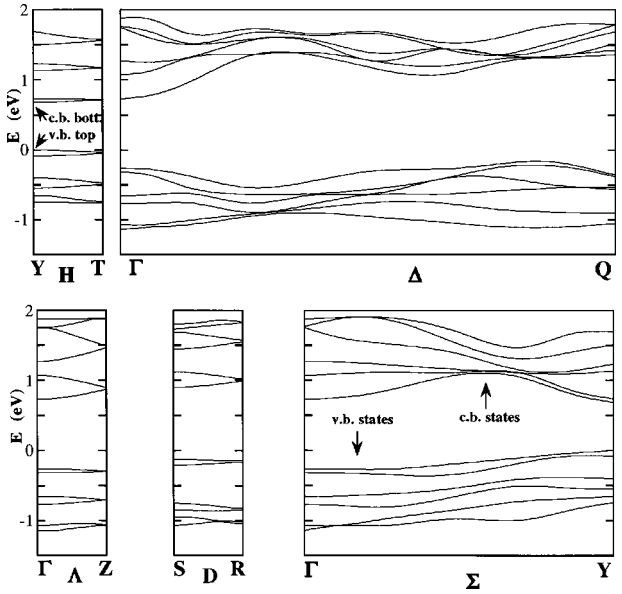

FIG. 5. Same as Fig. 4, but for $6\cdot$PbS-Bi_2S_3 (9,9), calculated within the single-cell virtual crystal approximation, using the relaxed measured coordinates and atomic ordering described by Eq. (2).

Bi_2S_3-Ag_2S superlattices the cutoff was increased to 6 Ry, in order to be consistent with Ref. 23.

IV. RESULTS AND DISCUSSION

A. $3\cdot$PbS-Bi_2S_3 and $6\cdot$PbS-Bi_2S_3

To check the validity of the virtual crystal approximation against the double-cell approach (with a single atom type at a site) we have made band-structure calculations of $3\cdot$PbS-Bi_2S_3 using both approaches. Results for the three configurations described by Eqs. (3)–(5) are given in Fig. 3, and those obtained by the single-cell virtual crystal approximation in Fig. 4. In both calculations the atomic coordinates were set to their measured relaxed values.[16] Different atomic configurations used within the double-cell approach give an uncertainty (i.e., variation of the calculated values) of the band gaps of ~0.2 eV. Similarly, energies of a few lowest conduction-band states or a few highest valence-band states, measured from the corresponding band extrema, show (dis)agreement ranging from almost zero to ~0.2 eV. On the other hand, the virtual crystal approximation within the single-cell approach and with the measured atomic ordering (1) was found to increase the band gaps at a few characteristic points by ~0.35 eV from the average values obtained in the double-cell approach. Also, the energies of neighboring states (measured from the corresponding band extrema obtained with single-cell calculation) differ by up to ~0.1 eV in respect to the average of double-cell values. For $6\cdot$PbS-Bi_2S_3 (9,9), which has a larger unit cell and hence requires a larger basis, the double-cell calculations were performed at a few k points only, and these results were found to agree with those obtained by virtual crystal approximation very much better, to within ~0.08 eV. We should also note that the effect of using the relaxed (measured) coordinates instead of idealized atomic coordinates leads to energy differences in the range ~0.1–0.2 eV in either approach. In

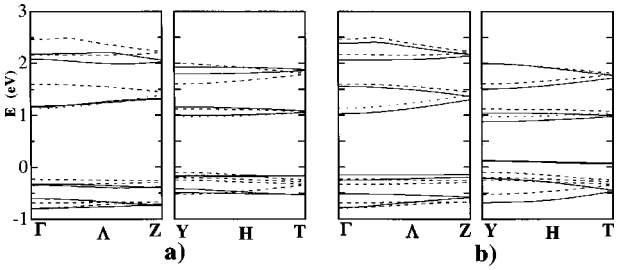

FIG. 6. Miniband structure along the Γ-Z and Y-T lines in $3\cdot$PbS-Bi_2S_3(6,6) calculated within the single-cell approach with idealized (dashed lines) instead of relaxed (solid lines) atomic coordinates (a), and with atomic ordering described by (10) (dashed lines) instead of (1) (solid lines), (b).

view of the fact that different local configurations should be expected to have different local relaxed coordinates (whose average is actually measured) we may conclude that, with the present level of knowledge on their structure and given the energy scales involved, the virtual crystal approximation should not be ruled out for calculating the electronic structure of PbS-Bi_2S_3–based superlattices. In fact, it seems quite accurate for the (9.9) case, so only this approach was used for the band-structure calculation of $6\cdot$PbS-Bi_2S_3. Results obtained that way, using the relaxed atomic coordinates and ordering described by Eq. (2) for $6\cdot$PbS-Bi_2S_3, are given in Fig. 5.

As displayed in Figs. 3–5, the highest filled and the lowest unfilled bands are well separated throughout the Brillouin zone, indicating that both of these structures are semiconductors. According to the virtual crystal approximation, Fig. 4, the top of the highest filled (valence) band in the (6,6) superlattice is at a point $k\approx 0.5(2\pi/a)$ away from Γ along the Δ line, and the bottom of the lowest empty (conduction) band at the Y point of the single-cell Brillouin zone [Fig. 2(a)]. This indirect band gap of 0.97 eV is, however, only marginally lower than the direct gap of 1.07 eV at the Y point. The double-cell calculations indicate that the band gap is probably lower by ~0.35 eV or so, and is indirect. As displayed on Fig. 3, for all three configurations explored the valence-band top is found at X and the conduction-band bottom at the Γ point of the double-cell Brillouin zone [Fig. 2(b)], the latter being the folded Y point of the single-cell Brillouin zone [Fig. 2(a)]. For the (9,9) superlattice extrema of both bands are at the Y point of Fig. 2(a), and the band gap is direct, amounting to 0.69 eV. Calculations at a few k points within the double-cell approach suggest that the band gap of $6\cdot$PbS-Bi_2S_3 could be lower by ~0.1 eV, and occurs at the Γ point of Fig. 2(b). In any case, the calculated band gaps are intermediate to the values for bulk PbS and Bi_2S_3 (i.e., 0.30 eV and 1.38 eV, respectively), but this may be somewhat accidental because Bi atoms here are in a different environment than in Bi_2S_3 crystal.

That the band gap of the (9,9) superlattice should be lower than that of (6,6) is what one would expect from simple superlattice considerations based on the content of PbS and the length of their periods (which, within the superlattice terminology, give, respectively, the ''bulk'' and ''quantization'' contributions to the total band gap). Such a trend, however, is clearly visible in single-cell (virtual crystal), but only marginally, if at all, in double-cell calculations.

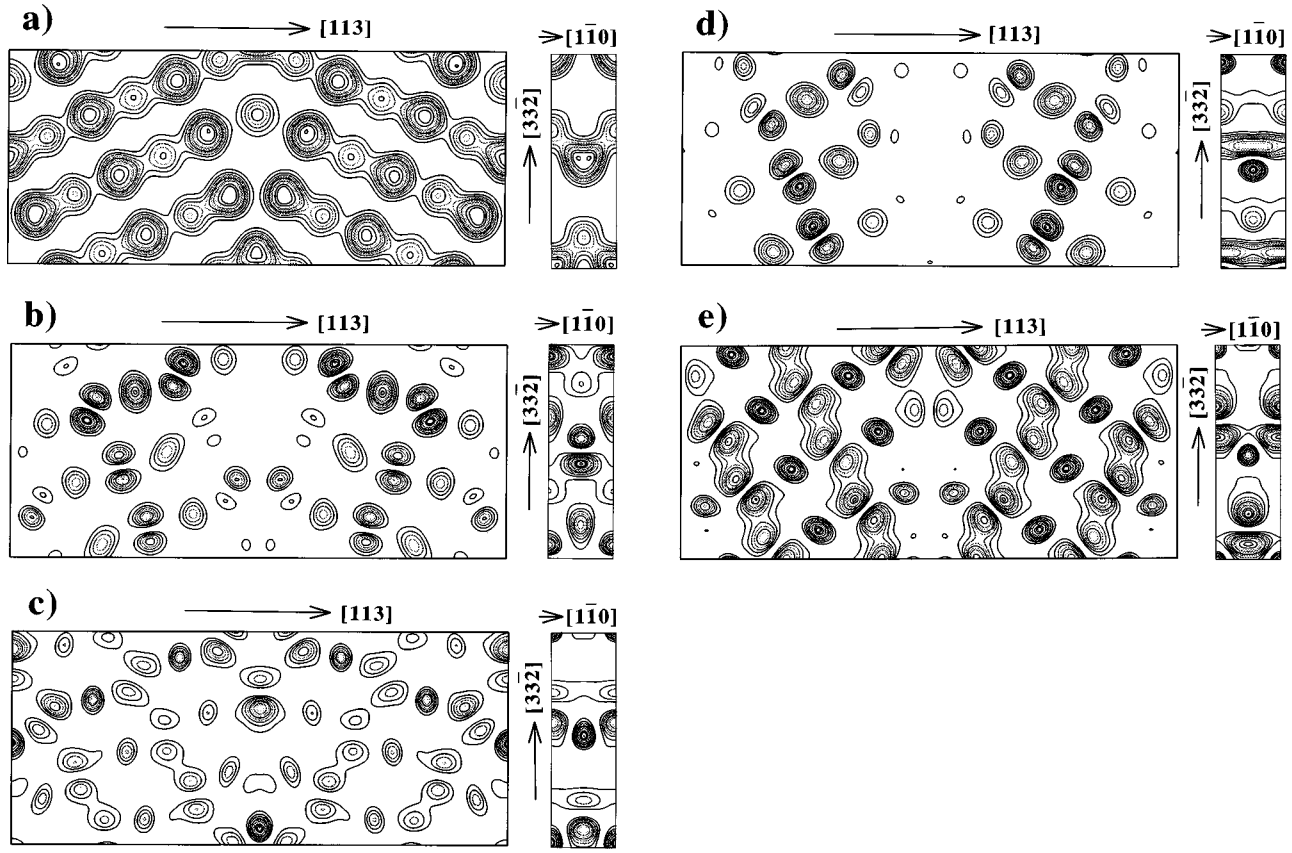

FIG. 7. Charge density plots on the $(1\bar{1}0)$ plane passing through the base-centered sulphur atoms of the (9,9) supercell (left), and on the (113) plane at the interface (right), for the total charge (a), valence-band top at Γ (b), conduction-band bottom at Γ (c), valence-band top at Y (d), and conduction-band bottom at Y (e). High-density regions in (a) correspond to S and lower density ones to Pb-Bi atoms.

Low dispersion in the superlattice growth direction and the presence of significant minigaps, typical for 2D systems, are present in both cases, but are more prominent in the (9,9) superlattice. These effects are due to both the symmetry mismatch of the two half-periods and the nonbulklike interface regions, which constitute significant ''barriers'' to electron transmission. Previous calculations for (111) twinning superlattices,[8,9] where the interface constitutes a rather mild perturbation of the crystalline potential, indicate that it is the interface region that is more responsible for quite wide minigaps.

The sensitivity of the band structure of $3\cdot$PbS-Bi_2S_3, calculated within the single-cell approach on atomic coordinates or on atomic ordering is given for a few examples in Fig. 6. While the precise knowledge of these may not be crucial in the somewhat simplified calculation as we have performed here, any more realistic study, say, within the multiple configurations double-cell approach, would have to use fairly precise data of this type.

The calculated charge density (total, and for a few individual states) on the (1 1 0) plane of the (9,9) supercell is given in Fig. 7. The bonding picture, as one can see from the total charge density in Fig. 7(a), is consistent with the ionic model, with a significant degree of covalency, which indicates the strength of the material, including the twinning interface. The atoms at the interface retain the sixfold coordination but with distorted bond angles, which is evident in Fig. 7(a) (right) for the (113) interface plane. Charge-density plots for individual states, Figs. 7(b)–7(e) (left), indicate that inside the bulk regions sulphur p orbitals contribute more to the valence, and metal s orbitals to the conduction states. On the interface, however, both of these orbitals contribute to either valence or conduction states, Figs. 7(b)–7(e) (right). The corresponding plots for the (6,6) case are quite similar to those given in Fig. 7, except for shorter bulk regions.

Finally, in Fig. 8 are given the (113) plane averaged charge densities for the three highest valence and three lowest conduction minibands at Γ and Y points of the Brillouin zone, as they vary along the (9,9) superlattice axis. The wave functions corresponding to various minibands in these structures are clearly more complicated than in many other semiconductor superlattices. The presence of nodes of the charge density at the interface for some of the bands indicates the strength of the scattering, and suggests that they are ''bulk related,'' while those that pile up at interfaces are more ''interface related.'' However, there seems to be no close relationship of such a classification with states affiliation to the valence or conduction bands.

B. $Pb_2Bi_6Ag_2S_{12}$ and $Pb_5Bi_6Ag_2S_{15}$

Band-structure calculations were also made for two of PbS-Bi_2S_3-Ag_2S–based structures, $Pb_2Bi_6Ag_2S_{12}$ (6,6) and $Pb_5Bi_6Ag_2S_{15}$ (6,9). Since the virtual crystal approximation cannot be safely used here, we have employed either the single-cell approach with particular atomic orderings, or the

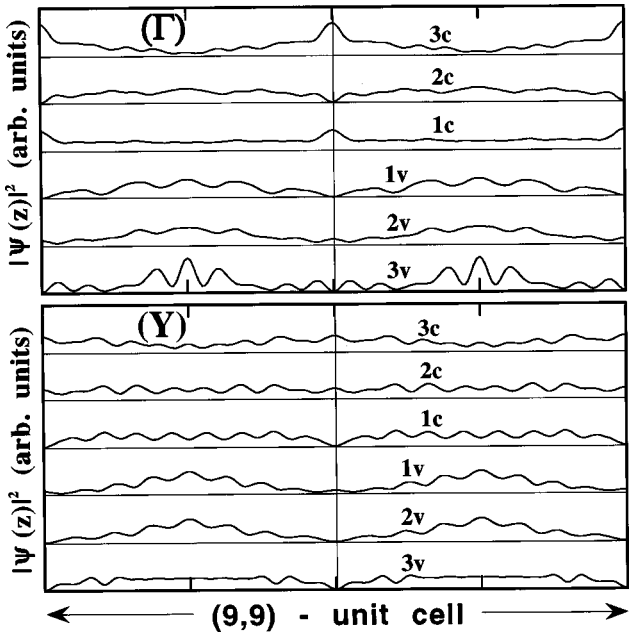

FIG. 8. Planar averaged charge density along the (9,9) superlattice growth direction [113] for the three highest valence and three lowest conduction-band states at Γ (top), and *Y* (bottom) points of the Brillouin zone.

double-cell approach. The overall band structure here turned out to be more sensitive to the type of calculation than is the case in PbS-Bi_2S_3–based superlattices.

A few examples of the calculated band structure of $Pb_2Bi_6Ag_2S_{12}$ within the single-cell approach are given in Fig. 9, and within the double cell approach in Fig. 10. Either way, the structure is predicted to be a semimetal. Based on data given in Figs. 9 and 10 and those for a few additional *k* points inside the Brillouin zone, the approximate positions of the Fermi levels are also denoted.

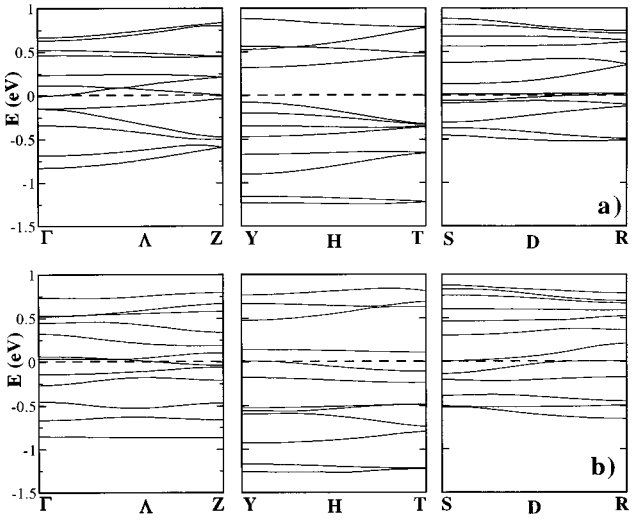

FIG. 9. Miniband structure along the Γ-*Z*, *Y*-*T*, and *S*-*R* lines in $Pb_2Bi_6Ag_2S_{12}$ (6,6) calculated with idealized atomic coordinates and metal atoms ordering $\widehat{\text{Pb}}$-Ag-Bi-Bi-Bi-$\widehat{\text{Pb}}$-Ag-Bi-Bi-Bi (a), and $\widehat{\text{Pb}}$-Ag-Bi-Bi-Bi-$\widehat{\text{Pb}}$-Bi-Bi-Bi-Ag (b), within the single-cell approach. Approximate position of the Fermi level, also used as a zero-energy reference (dashed lines) is also denoted.

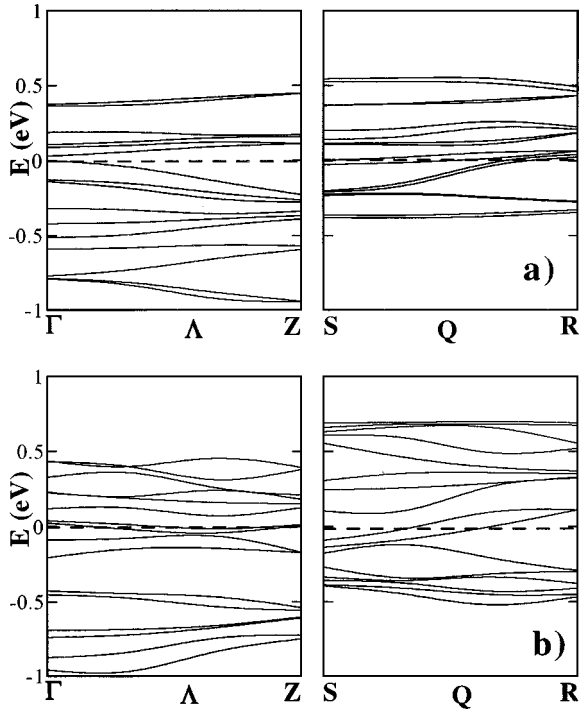

FIG. 10. Miniband structure along the Γ-*Z* and *S*-*R* lines in $Pb_2Bi_6Ag_2S_{12}$ (6,6) calculated with idealized atomic coordinates and metal atoms ordering given by Eq. (8) (a), and (9) (b), within the double-cell approach. Approximate positions of the Fermi level (dashed lines) are also denoted.

For $Pb_5Bi_6Ag_2S_{15}$ (6,9) only the single-cell approach was used, and the calculated dispersion along the Γ-*Z* line is given in Fig. 11. Based on this single calculation, $Pb_5Bi_6Ag_2S_{15}$ is also likely to be a semimetal. Figures 9 and 10 suggest that the calculations for $Pb_5Bi_6Ag_2S_{15}$ should better have been done within the double-cell approach, but, in view of the larger cutoff energy required by Ag, this was beyond our computational resources.

For other PbS-Bi_2S_3-Ag_2S superlattices with even longer periods, we have yet to perform calculations, because neither their relaxed atomic coordinates nor the atomic ordering have been determined. It is likely that for some of them even the double-cell approach would not suffice to achieve a single atom type at a site, and reconstructed cells should be used for this purpose. In view of still lacking any experimental guidance such calculations would presently be of doubtful usefulness.

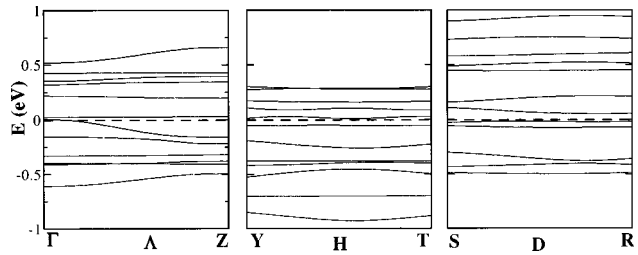

FIG. 11. Miniband structure in $Pb_5Bi_6Ag_2S_{15}$ (6,9) calculated within the single-cell approach, with relaxed atomic coordinates (Ref. 20) and metal atoms ordering $\widehat{\text{Pb}}$-Ag-Bi-Bi-Bi-$\widehat{\text{Pb}}$-Ag-Bi-Pb-Pb-Bi-Bi. Approximate position of the Fermi level (dashed line) is also denoted.

V. CONCLUSION

We have made the empirical pseudopotential calculation of the band structure of natural, self-organized twinning superlattices based on PbS-Bi_2S_3 and PbS-Bi_2S_3-Ag_2S alloys. The former are predicted to be semiconductors and have the subband structure resembling that found in the conventional superlattices, with quite sizable minigaps. The two variations of the latter that were explored ($Pb_2Bi_6Ag_2S_{12}$ and $Pb_5Bi_6Ag_2S_{15}$) are both predicted to be semimetals. Since the fabrication of chemical twinning superlattices is far less demanding technologically than that of conventional superlattices, it is hoped that this first attempt to calculate their band structure will attract further theoretical and experimental research on their properties and applications.

Considering the semiconductors first, the fact that only two stable phases exist in the PbS-Bi_2S_3 system does limit the versatility of these structures, but, on the other hand, this could be considered as a distinct advantage: the interfaces are perfectly flat, with no interface roughness taking place (this feature is nicely displayed in micrographs presented in Ref. 14), and with apparently no significant interdiffusion. While polytype superlattices and (111) twinning superlattices could also be free of interface roughness problems,[6] the stability of the superlattice period may not always be guaranteed. On the other hand, the (113) chemical twinning superlattices, by the very nature of their formation, are expected to be very stable structures, since the superlattice ordering of the alloy seems to be energetically favorable, and rather insensitive to the details of the growth method and to the presence of impurities. Some amount of fine tuning of the band structure may be achieved through appropriate isovalent substitutions, e.g., replacing some of the sulphur by (Se,Te), or some of Bi by Sb, etc., as occur in the composition of natural minerals of this type.[14,18] This kind of tunability does have limits, however, because highly or fully substituted crystals may have a different and more complex structure than the twinning superlattices.[26] Nonisovalent impurities, also occurring in minerals, constitute their natural dopants, leading to the possibility of artificial doping of grown crystals.

Still remaining to be explored is the band structure of PbS-Bi_2S_3-Ag_2S and PbS-Bi_2S_3-Cu_2S superlattices other than the two types we have dealt with here. Some further measurements of atomic ordering in them, or their electronic or optical properties, would definitely be very helpful for refinement of the rather simplified model we have here employed. It would also be interesting to explore the possibility of obtaining different periodicities (other than the two observed in PbS-Bi_2S_3, for instance), by employing the molecular-beam epitaxy technique. Giving up the self-organization aspect, while retaining the interface stability, may significantly extend the band-engineering capabilities of these structures.

ACKNOWLEDGMENTS

The authors would like to thank the EPSRC (U.K.) for computational facilities through the CSI scheme. One of the authors (Z.I.) is grateful to the Royal Society (U.K.) for financial support.

[1] G. P. Srivastava, J. L. Martins, and A. Zunger, Phys. Rev. B **31**, 2561 (1985).
[2] K. A. Mäder and A. Zunger, Phys. Rev. B **51**, 10 462 (1995).
[3] A. Mascarenhas, R. G. Alonso, G. S. Horner, S. Froyen, K. C. Hsieh, and K. Y. Cheng, Phys. Rev. B **48**, 4907 (1993).
[4] S. P. Ahrenkiel, S. H. Xin, P. M. Reimer, J. J. Berry, H. Luo, S. Short, M. Bode, M. Al-Jassim, J. R. Buschert, and J. K. Furdyna, Phys. Rev. Lett. **75**, 1586 (1995).
[5] S. Y. Ren and J. D. Dow, Phys. Rev. B **39**, 7796 (1989).
[6] F. Bechstedt and P. Käckell, Phys. Rev. Lett. **75**, 2180 (1995).
[7] Z. Z. Bandić and Z. Ikonić, Phys. Rev. B **51**, 5806 (1995).
[8] Z. Ikonić, G. P. Srivastava, and J. C. Inkson, Phys. Rev. B **48**, 17 181 (1993); Solid State Commun. **86**, 799 (1993).
[9] Z. Ikonić, G. P. Srivastava, and J. C. Inkson, Phys. Rev. B **52**, 13 734 (1995).
[10] K. Hiruma, M. Yazawa, K. Haraguchi, K. Ogawa, T. Katsuyama, M. Koguchi, and H. Kakibayashi, J. Appl. Phys. **74**, 3162 (1993).
[11] Z. Ikonić, G. P. Srivastava, and J. C. Inkson, Phys. Rev. B **55**, 9286 (1997).
[12] R. L. Headrick, B. E. Weir, J. Bevk, B. S. Freer, D. J. Eaglesham, and L. C. Feldman, Phys. Rev. Lett. **65**, 1128 (1990).
[13] R. J. D. Tilley and A. C. Wright, Chem. Scr. **19**, 18 (1982).
[14] A. Skowron and R. J. D. Tilley, J. Solid State Chem. **78**, 84 (1989); **85**, 235 (1990).
[15] H. H. Otto and H. Strunz, N. Jb. Miner. Abh. **108**, 1 (1968).
[16] J. Tagaki and Y. Takeuchi, Acta Crystallogr., Sect. B: Struct. Crystallogr. Cryst. Chem. **28**, 649 (1972).
[17] Y. Takeuchi and J. Takagi, Proc. Jpn. Acad. **50**, 76 (1974).
[18] E. Makovicky and S. Karup-Moller, N. Jb. Miner. Abh. **130**, 264 (1977); **131**, 56 (1977).
[19] K. Aizawa, E. Iguchi, and R. J. D. Tilley, J. Solid State Chem. **48**, 284 (1983).
[20] E. Makovicky, W. G. Mumme, and I. C. Madsen, N. Jb. Miner. Abh. **H10**, 454 (1992).
[21] S. E. Kohn, P. Y. Yu, Y. Petroff, Y. R. Shen, Y. Tsang, and M. L. Cohen, Phys. Rev. B **8**, 1477 (1973).
[22] J. Rose and R. Schuchardt, Phys. Status Solidi B **117**, 213 (1983); *ibid.* **139**, 499 (1987).
[23] Y. Yamada, Phys. Status Solidi B **102**, 629 (1980).
[24] C. Y. Fong, J. P. Walter, and M. L. Cohen, Phys. Rev. B **11**, 2759 (1975).
[25] C. J. Bradley and A. P. Cracknell, *The Mathematical Theory of Symmetry in Solids* (Clarendon, Oxford, 1972).
[26] R. J. D. Tilley and A. C. Wright, J. Solid State Chem. **64**, 1 (1986).